

Data-driven tool wear prediction in milling, based on a process-integrated single-sensor approach

Eric Hirsch and Christian Friedrich¹

Abstract—Accurate tool wear prediction is essential for maintaining productivity and minimizing costs in machining. However, the complex nature of the tool wear process poses significant challenges to achieving reliable predictions. This study explores data-driven methods, in particular deep learning, for tool wear prediction. Traditional data-driven approaches often focus on a single process, relying on multi-sensor setups and extensive data generation, which limits generalization to new settings. Moreover, multi-sensor integration is often impractical in industrial environments. To address these limitations, this research investigates the transferability of predictive models using minimal training data, validated across two processes. Furthermore, it uses a simple setup with a single acceleration sensor to establish a low-cost data generation approach that facilitates the generalization of models to other processes via transfer learning. The study evaluates several machine learning models, including convolutional neural networks (CNN), long short-term memory networks (LSTM), support vector machines (SVM) and decision trees, trained on different input formats such as feature vectors and short-time Fourier transform (STFT). The performance of the models is evaluated on different amounts of training data, including scenarios with significantly reduced datasets, providing insight into their effectiveness under constrained data conditions. The results demonstrate the potential of specific models and configurations for effective tool wear prediction, contributing to the development of more adaptable and efficient predictive maintenance strategies in machining. Notably, the ConvNeXt model has an exceptional performance, achieving an 99.1% accuracy in identifying tool wear using data from only four milling tools operated until they are worn.

Index Terms—Tool Wear Prediction, Signal Analysis, Machine Learning, Deep Learning, Milling, Vibration, Tool Condition Monitoring, Accelerometer.

I. INTRODUCTION

Economically, optimizing tool change times and extending tool life are essential to minimize downtime and maximize output, reducing overall operating costs. A primary concern in this domain is tool wear, which represents a challenge within the machining industry. At present, tool wear is primarily based on supplier recommendations and manual expertise [1]. However, because numerous factors influence tool wear during machining, its behavior is highly complex and variable, making it difficult to predict accurately using conventional or heuristic methods. So tool wear still occurs, often leading to disruptions in the manufacturing process. Ineffective management of tool wear,

whether through premature or delayed identification, can result in a number of unwanted consequences, including unnecessary replacement costs and poor product quality [2]. Therefore, comprehensive research and development of intelligent tool condition monitoring (TCM) systems [3]–[5] is essential. TCM systems estimate the tool condition by passing sensor inputs through defined models, assisting machine operators in optimizing their work practices. The tool condition is characterized either through categorical classification, indicating distinct wear states, or through regression to estimate the wear condition. For regression, flank wear is usually applied as a measured variable, which is attempted to be predicted.

TCM can operate offline or online [6]:

- Offline TCM, predictions are made post-process using additional data sources, which may include direct measurement methods. Tool wear is only identified with a significant delay or the process must be temporarily interrupted.
- Online TCM offers the process to be continuously evaluated without interrupting the process. This enables short-interval or real-time updates on tool wear. Indirect measurement methods are typically the only viable option in online TCM.

Indirect measurement methods of tool wear, such as force/torque, acceleration, temperature, motor currents, and acoustic sensors [7], produce data that must be processed and analyzed using intelligent models to gain interpretable insights. In contrast, direct measurement techniques, including image recognition, optical measurements and durability assessments, offer more straightforward data interpretation. The indirect method, or online TCM, requires no downtime and is therefore the preferred approach in many studies. Research in this area typically falls into two categories: physic-based models [8] and data-driven models [9]. Physic-based models offer detailed theoretical explanations and mechanism analysis, such as monitoring force modeling coefficients during cutting to track tool wear. However, due to the complex non-linear nature of cutting processes, it is difficult to parameterize and some effects, such as cutting temperature or lubrication conditions, are ignored to simplify the model. This limits the accuracy of the model when there is no clear physical mechanism. As a subset of Industry 4.0, rapid advances in computing, digitization and artificial intelligence (AI) have made it easier to implement data-driven models. These models use deep learning techniques, a subset of machine learning, to correlate

¹ All authors are with the Institute of Applied Research, Karlsruhe University of Applied Sciences (HKA), Germany, {eric.hirsch, christian.friedrich}@h-ka.de

sensor readings with tool wear, eliminating the need for a deep understanding of the physical processes. This enables faster implementation of TCM's and makes data-driven approaches more accessible to diverse machining configurations, which is why this study used a data-driven method.

II. RELATED WORK

The paper employs a single acceleration signal to generate training data for data-driven models. This decision is motivated by the challenges associated with multi-sensor setups, such as the inability to integrate all sensors into every machine and the high costs or time requirements associated with sensor integration. These challenges hinder the generalization of results of multi-sensor setups across diverse applications.

To provide context for the single-sensor approach, we still introduce several multi-sensor systems (MSS) as a basis for comparison. A multi-sensor system has the advantage of combining diverse sensor types and thus different signal inputs. In addition, the same sensor type can record data at different positions, typically near the tool, the workpiece, or the spindle to capture specific aspects of the milling process. One approach in multi-sensor systems is to focus on a single area, similar seen in simpler sensor setups. In some studies, sensor placement focuses solely on the spindle, measuring spindle vibrations across multiple axes, spindle current, spindle force and the machine's axis positions [10]. Other studies focus on the workpiece, using a stationary dynamometer under the workpiece (a "force plate") with additional sensors for vibration and spindle current monitoring in different positions [11].

However, most papers employ a multi-sensor approach by distributing sensors at various locations. These setups often use a force plate as the primary data source, supplemented by additional sensors for vibration and current measurements positioned elsewhere on the machine [12]. With multi-sensor setups, the data volume is inherently larger and can be further enhanced by adding a few hand-crafted features for training data-driven models. Various model architectures have been applied in MSS research, including random forest [13], support vector machines [14], simple neural networks [15] and convolutional neural networks (CNN) [16]–[18]. Among these, long short-term memory (LSTM) networks are frequently used due to their ability to handle time-series data [19], [20]. A common limitation across these MSS-based studies is the invasive machine modifications needed to install sensors, which often require specialized setups and time-consuming sensor installation and removal. Consequently, these studies are typically limited to testing on a single machine or using publicly available datasets [21]–[23] that were originally employed in a competitive context. Most public datasets still consist of data from only one machine.

In contrast to multi-sensor systems, the following studies employ minimalistic sensor setups, utilizing only one sensor or a few single-axis sensors positioned at the same location to simulate the functionality of a 2- or 3-component sensor. Sensors are strategically placed as close to the machining process as possible. Commonly, they are placed either near the workpiece or near the toolholder, though a placement near the spindle is occasionally used. When placed near the toolholder, the sensors are integrated directly into the toolholder or attached as adapters between the toolholder and the spindle. Typical sensor choices include 3-component dynamometers, such as the force plate [24], and accelerometers, as these offer valuable insight into the dynamics of processes and machines through frequency analysis. Because simple sensor setups yield only one type of data, additional processing is often required to improve interpretability. This is achieved by supplementing the data with process parameters or generating handcrafted features. Common handcrafted features include statistical measures such as arithmetic mean, variance, skewness, and kurtosis [25]. Another popular approach involves data transformation techniques. For example, Zhang et al. apply wavelet packet decomposition to enrich data content, followed by an autoencoder for further processing [26]. Another study employs variable mode decomposition (VMD) to extract meaningful signal features [27]. Popular models for TCM with simple sensor setups include deep neural networks (DNN), convolutional neural networks (CNN) [28], and long short-term memory (LSTM) networks [29]. For 2D CNN's, data must be transformed into an image-like format, either by concatenating time-series features into a matrix or through frequency-time transformations such as the Continuous Wavelet Transform (CWT) or the Short Time Fourier Transform (STFT), which offer a time-frequency perspective on the data.

Overall, these studies demonstrate promising results within their specific use cases, showing that models can identify correlations between sensor measurements and tool wear. However, model validation has typically been limited to a single milling process, with only variations in the process parameters. As a result, while the models were proven capable of capturing wear-related patterns in this context, their ability to generalize or identify universal patterns in wear behavior, remains largely unexplored. Another limitation is that most studies conducted milling processes in a dry state to accelerate wear. In industrial applications, milling is often performed with a cooling lubricant, which affects tool wear differently. This discrepancy between experimental conditions and real-world practices makes it challenging to assess how well these research findings would translate to most industry applications.

In this study, we will address the limitations observed in previous research. As a result, this study makes the following contributions:

- Employment of a cost-effective data-driven approach for the rapid implementation of TCM's.
- Utilization of a single accelerometer sensor, which is straightforward to integrate into a range of machines and processes
- Validating the model's generalization capabilities and the necessity of retraining by performing wear prediction on two machines.
- Identification of the minimum amount of training data required, thereby reducing the burden of data collection.
- Comparison of multiple model architectures, including a ConvNeXt model, LSTM, decision tree and support vector classifier (SVC).

III. ARCHITECTURE DESIGN FOR WEAR PREDICTION

A. Problem description and Pipeline

Data-driven models require large datasets to capture the non-linear relationships and random variations inherent in complex machine processes. In addition, these models are often tailored to the specific processes they are trained on. In a real world applications, however, processes can frequently change, and for companies to justify the investment in wear detection systems, these models need to be adaptable to new or evolving processes. The complexity of tool wear makes it challenging to develop a generalizable data-driven model that can apply across various processes, limiting the practical implementation of such research. To address this issue, this paper proposes a different approach by comparing various data-driven models and evaluating their performance based on the quantity of available training data. The training data is based on a single acceleration sensor, enabling fast and cost-effective model training for any process. It also makes it easier to adapt the model to new processes, making it more suitable for transfer learning. The training datasets contain acceleration data of vibrations during the milling process. From these raw signal transformed entities, relevant features are extracted with the objective of predicting tool wear. The problem is framed as a binary classification task, with the aim of determining if wear with a negative impact is present.

B. Data preprocessing

The accelerometer generates a continuous stream of acceleration data \ddot{x} that includes not only the critical process information related to tool wear, but also all the surrounding recordings, such as spindle run-up, tool change and the transitional moments when the tool is starting or finishing its milling operation. To filter out these unwanted data, the signal is automatically processed by analyzing its peak-to-peak (\ddot{x}_{p2p_t}) over time steps t with a moving window of length w .

$$\ddot{x}_{p2p_t} = \max(\ddot{x}_{t-w+1}, \ddot{x}_{t-w+2}, \dots, \ddot{x}_t) - \min(\ddot{x}_{t-w+1}, \ddot{x}_{t-w+2}, \dots, \ddot{x}_t) \quad (1)$$

A threshold is calculated to isolate the segments of the signal that correspond to the actual milling process. For this, the \ddot{x}_{p2p_t} curve is sorted in ascending order (\uparrow) and then the average lowest value m_{p2p} is determined as described below. Here N is the length of the \ddot{x}_{p2p_t} curve.

$$m_{p2p} = \frac{1}{N} \sum_{i=\alpha_0 \cdot N}^{\alpha_1 \cdot N} \ddot{x}_{\uparrow p2p_i}, \quad (2)$$

$$th = \alpha_2 \cdot m_{p2p} \quad (3)$$

The $\alpha_0 - \alpha_2$ represent empirically determined values: $\alpha_0 = 0.01$, $\alpha_1 = 0.03$, $\alpha_2 = 10$. The signal is also trimmed according to the duration for which it is below or above the threshold th , thereby preventing the misclassification of brief anomalies with comparable vibration energy. The data preprocessing is explained in Fig. 1.

C. Feature engineering

The acceleration data takes a measurement every $65 \mu s$, giving a sampling rate of approximately 15,38 kHz. This leads to a Nyquist border with 7,89 kHz, so the data theoretically contains a large amount of information. Nevertheless, the data is derived from only a one-dimensional acceleration signal, posing a challenge in identifying the complete range of characteristics and correlations related to wear. To address this, several techniques have been developed to improve the interpretability of the signal for the model, often by reducing the amount of data while preserving the essential information. One such approach is signal transformation, where the signal can be analyzed in different domains: time domain, frequency domain, or time-frequency domain. In this paper, the Fourier or Welch transformation is used to transfer the signal in the frequency domain and the STFT for the time-frequency domain. As a result, the original one-dimensional signal is transformed into a multi-dimensional input for the model. Fig. 2a shows the different data transformations on the left. Optionally, the input can be further adjusted to reduce the input size. This is done by extracting features. Popular features are typical statistical features such as mean, peak-to-peak, kurtosis, and skewness. However, there are also special or self-developed features that are used in this paper. The most important features are listed in Table I.

D. Different models

Fig. 2a illustrates the structure of the models. First, there is the input, followed by the type of feature extraction (i, ii) and the classifier used (1, 2, 3, 4). The first type of feature extraction (i) is a model backbone. In this work, an advanced and modern CNN architecture, the ConvNeXt architecture [30], is selected as the backbone. This model builds upon the

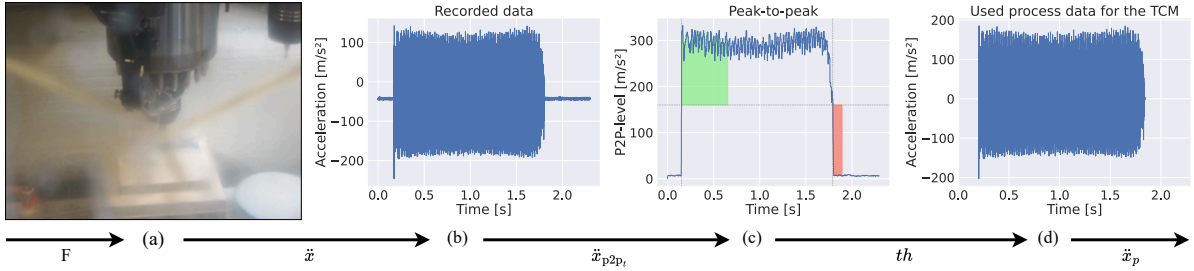


Fig. 1: Pipeline for generating process data: (a) The milling force is converted into acceleration data \ddot{x} . (b) A plot of the recorded acceleration data is shown. (c) The result of the p2p function \ddot{x}_{p2p_t} is displayed, along with the duration (green or red areas) where \ddot{x} exceeds or falls below the threshold th . Using this analysis, the acceleration data is segmented into process data (d). The resulting process data \ddot{x}_p is used for our classification pipeline.

successful ResNet framework [31] and incorporates enhancements inspired by modern model architectures like the Swin Transformer [32]. Benchmark studies have demonstrated that this model is at least as effective as the Vision Transformer [33]. In the Model "ConvNeXt", wear is predicted from the extracted features of the STFT with fully connected layers (1). In the model "ConvNeXtLSTM", a sequence of features is extracted from a sequence of STFT's and processed with LSTM's to subsequently predict wear with fully connected layers as well (2).

In the second type of feature extraction (ii), features are derived from the acceleration data using proprietary algorithms, producing a feature vector of 20 selected features as input. This feature vector is utilized by the model "SVC" with a Support Vector classifier (3) and by the model "DTreeC" with a decision tree classifier (4). Fig. 2b shows the different models in detail.

E. Training and Evaluation process

The training data is organized in such a way that multiple process runs are performed for each milling operation. Each run tracking the entire tool life cycle of a tool: from completely new to completely worn out. During model training, it is critical to avoid random splitting of the data between training and validation sets, as this can lead to mixing of process runs. This is because each run contains a new tool with different wear behavior, making random splitting inappropriate. To ensure a valid model evaluation, no part of a specific process run should be used in both training and validation. If the model is exposed to segments of the same run in both phases, it may overfit to the specific wear patterns of that particular run rather than learning to generalize across different tools and wear conditions. Fig. 3 shows how the data is sorted in training data and validation data.

Two milling machines are utilized for the training and evaluation process. The first machine generates the training and validation data for the various models. It has a smaller working area and is therefore more resistant. To assess model performance with minimal training data, we iteratively train each model with

a decreasing number of process runs. This method allows us to evaluate how the model behaves with both rich and limited data, revealing which models are more robust with larger datasets and which perform better under data-constrained conditions. We also determine the minimum amount of training data required to achieve acceptable performance and the amount necessary for optimal results. The next step is to assess how effectively the models trained on one process generalize to a different, yet similar, process. For this purpose, the milling machine is changed. This second machine is optimized for multifunctional machining but exhibits lower stability. It is important to acknowledge that the two machines used in this study exhibit fundamentally distinct dynamic behaviors. Throughout the evaluation, the models are compared to determine their effectiveness in handling new unseen processes and to detect their relative strengths and performance differences.

IV. EXPERIMENTAL RESULTS

A. Setup

For this experiment, the tool life cycle of a solid carbide square end mill with four teeth and a diameter of 12 mm is analyzed on two different machines: the first machine is the 'CHIRON FZ 15 S' and the second machine the 'DMU 60 FD duoBLOCK'. The workpiece material is hardened steel (42CrMo4, +QT), chosen for its demanding properties. The toolholder and sensor used for the experiment is the 'iTENDO2' from Schunk, which integrates a sensor directly into the center of the toolholder housing (Fig. 4a). The sensor used is a single-axis MEMS acceleration sensor that measures radial acceleration (a_r). As the sensor is placed on the rotation axis of the toolholder, it is able to effectively measure the acceleration on the x-axis (a_x) and y-axis (a_y) over time, as it rotates with the toolholder and spindle speed. Fig. 4b illustrates the measurement behavior, which presents a top view of the iTENDO2 in the xy plane with the axis of rotation being the z-axis. A rotation matrix is applied to calcu-

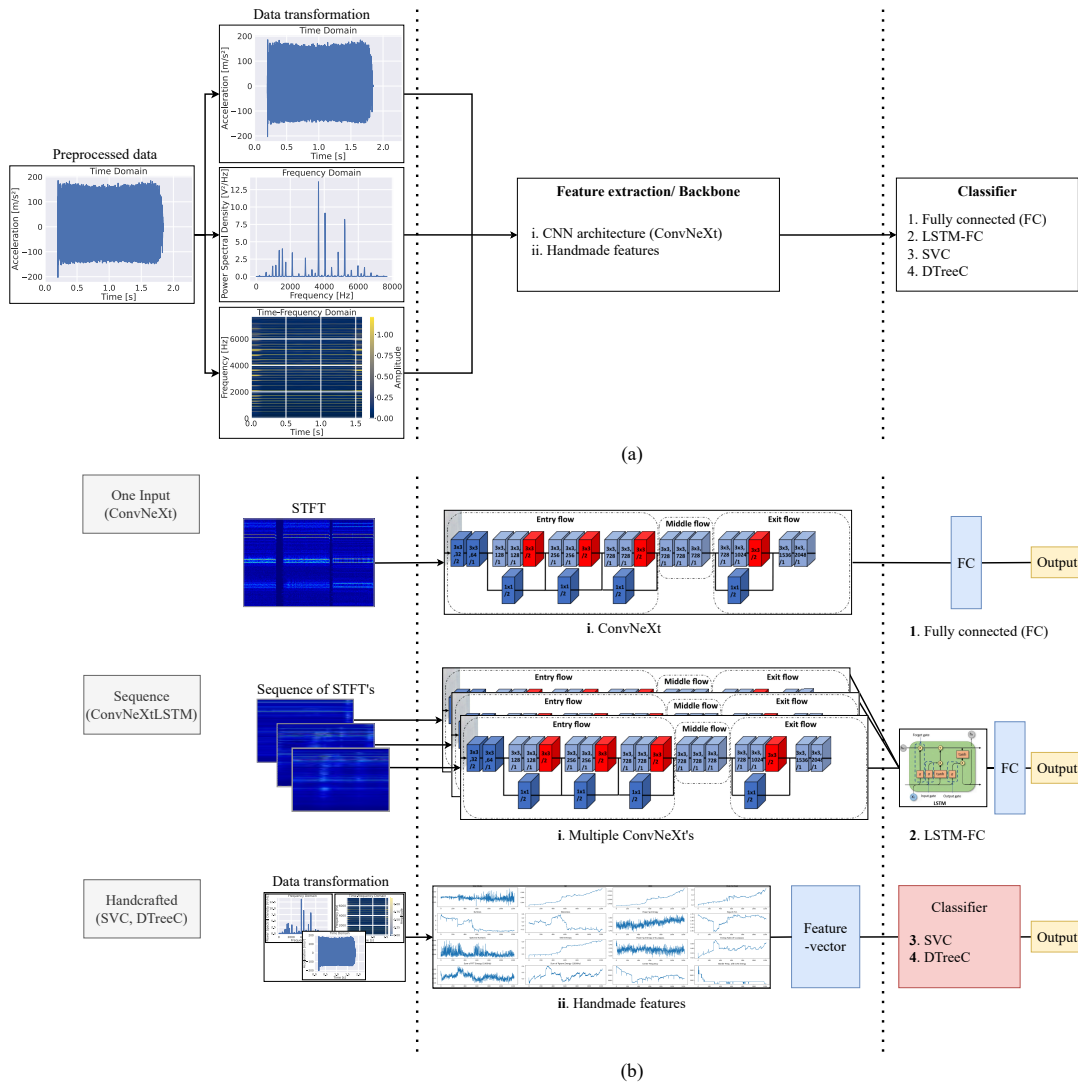


Fig. 2: (a) The diagram illustrates the transformation of acceleration data into different domains and the subsequently extraction of features using either a CNN architecture (i) or proprietary algorithms (ii). These features are then utilized by various classifiers (1, 2, 3, 4) to predict wear. (b) The architectures of the four classifiers used in this paper, categorized by their input type, are shown. Images from the following sources were used to create this diagram: [34], [35]

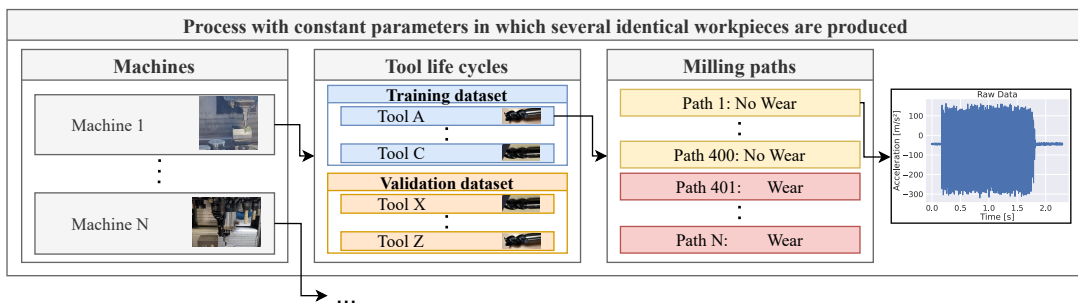


Fig. 3: Structure of the datasets used for the models: Each process dataset includes multiple machines, and each machine dataset contains several tool life cycles. A single tool life cycle represents the use of one tool until it becomes worn. Within each dataset, multiple workpieces are produced.

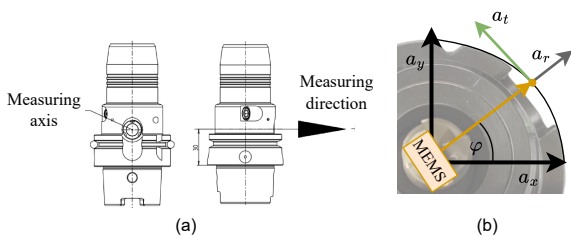


Fig. 4: (a) Side view of the toolholder with the integrated 1-axis MEMS sensor. (b) Top-down view of the toolholder, illustrating how the sensor measures acceleration in the xy -plane, depending on the rotation angle φ .

late a_r , accounting for the changing contributions of a_x and a_y based on the rotation angle φ :

$$\begin{bmatrix} a_r \\ a_t \end{bmatrix} = \begin{bmatrix} \cos(\varphi)a_x + \sin(\varphi)a_y \\ \cos(\varphi)a_y - \sin(\varphi)a_x \end{bmatrix} \quad (4)$$

If the sensor is installed optimally, it does not measure tangential acceleration a_t . As a result, the measured accelerations are dynamically mixed depending on the angle of rotation, enriching the signal with more detailed acceleration information. However, this also makes the signal more challenging to interpret. The reason for this is that the rotation matrix multiplies frequencies in the time domain, as both a_x and a_y also consist of frequency components. In accordance with the convolution theorem, the frequencies in the frequency domain are also convolved. This particular sensor/toolholder combination is still chosen because the sensor's position allows it to capture undamped process vibrations more effectively. In addition, the setup is easily transferable to other machines and processes, requiring only the replacement of the toolholder to record training data under similar conditions. This modularity aligns seamlessly with the key contribution of this research: the development of a novel TCM pipeline that enables models to be swiftly adapted to a range of industrial milling processes for wear classification.

B. Design of Experiment

In this experiment, a flat surface is created on a metal block using side milling. This milling process is repeated continuously until the cutting tool shows significant wear. The milling operation is a down-milling approach, with coolant lubricant applied throughout the process. Milling is performed exclusively along the xy plane. Detailed process parameters are given in Table II and the visualization of the experiment is shown in Fig. 5. In order to accurately characterize the acceleration data, the flank wear of the end mill is measured at regular intervals. When the flank wear reached 0.2 mm, the tool is considered to be highly worn, indicating the completion of one tool life cycle and the process run restarts with a new tool. In addition to direct measurement, the machine operator provides

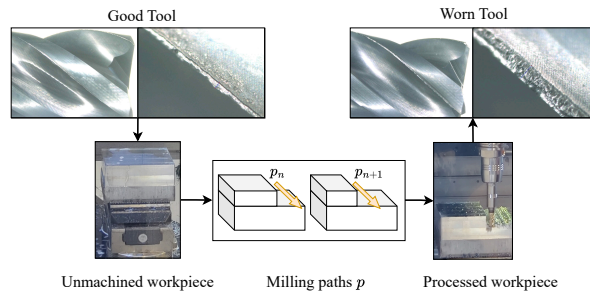


Fig. 5: Procedure for one tool life cycle, involving machining N milling paths until the tool becomes excessively worn.

a subjective label based on their experience. This label is the tool state, indicating when the tool wear had reached a level where the negative impact on the process becomes too great. The tool state is used for wear prediction in this research.

V. EVALUATION

Each model is trained and validated using the Chiron machine dataset. The ratio of training data to validation data is divided into four steps. It starts with 20% training to 80% validation and changes the ratio in steps of 20% up to the ratio of 80% training to 20% validation. A total of 30 models per architecture are trained across all four splits. Each model is trained over a maximum of 16 epochs, with often only a slight improvement in model performance observed from epoch 12 onward. The model weights that performed best on the validation dataset are used. Fig. 6 shows the accuracy of each model architecture as a heatmap over the amount of training data. It can be seen that

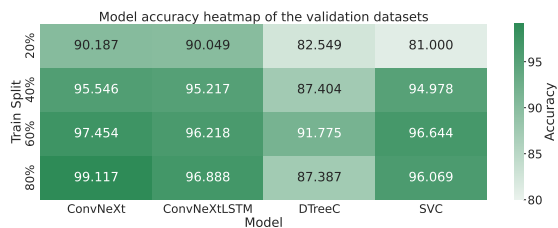


Fig. 6: A heatmap showing the accuracy of various trained models on the validation datasets.

there are only small differences between the training data of 80% and 60%. This indicates that a good prediction of machine wear can be achieved by training on 60% training data, which corresponds to three tool life cycles. In addition, we see that the first group, using the STFT as input, performs better. However, due to the larger number of parameters and the deeper architecture, these models have a higher computational cost and memory requirement. Although the prediction accuracy or binary accuracy reflects the overall quality of the model, in reality it is more important how the model predicts wear over time, in particular when the model changes its prediction from not worn to

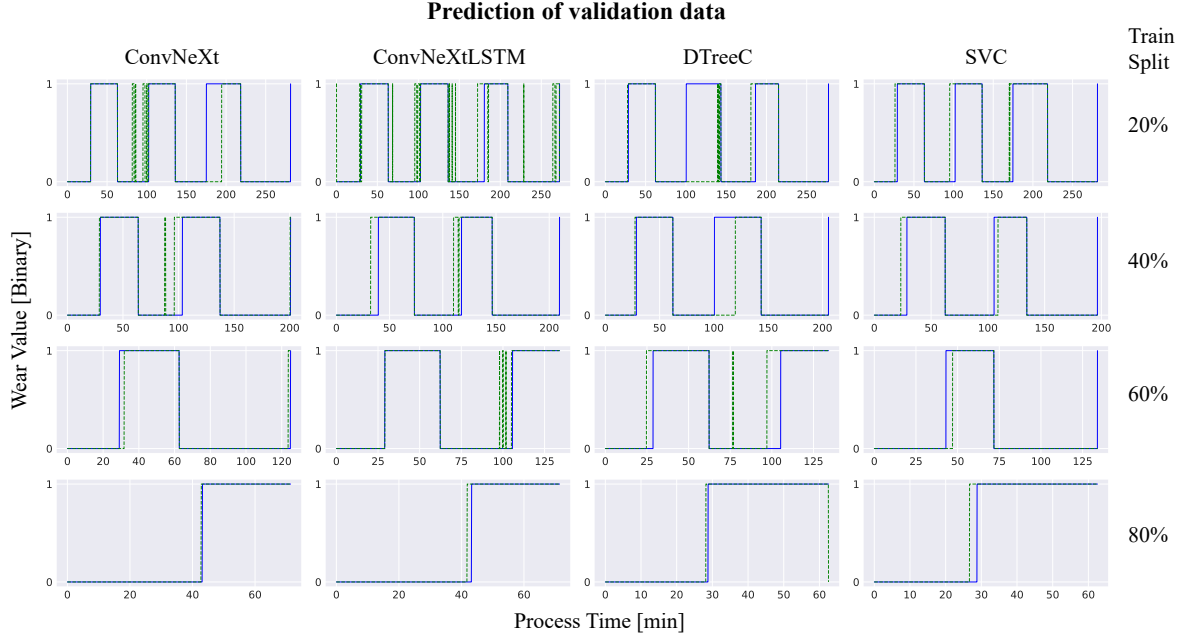


Fig. 7: The time-based wear predictions of the various models, which have been trained on different amounts of data. The dashed green line represents the model’s predictions, while the blue line indicates the true labels.

worn. Fig. 7 shows the prediction of wear over time. The y-axis illustrates the categories of the binary classification, which are defined as follows:

$$C : \{0, 1\} \rightarrow \{\text{Not worn}, \text{Worn}\} \quad (5)$$

The wear subjectively labeled by the operator (true label) is shown in blue and the model prediction is shown in green. Depending on the plot, several tool life cycles are shown concatenated in one plot. When the label changes from Worn to Not worn, a new tool life cycle begins. For post-processing, a simple filter is applied to the classification results to address the logical inconsistency that a tool cannot briefly appear worn and then revert to an unworn state. This filter eliminates a small proportion of such outliers from the plots, thereby enhancing both the accuracy over time and the readability of the visual representations. However, prominent outliers remain visible in the plots. Fig. 7 illustrates that time accuracy improves as the size of the training set increases. It is noteworthy that certain models, such as ”ConvNeXt”, demonstrate relatively good time accuracy even with only 40% of the training data. The ”SVC”, despite its simplicity, achieves only slightly lower time accuracy compared to more advanced models. The results together demonstrate that a minimum of two, preferably three, tool life cycles is required to train a model with the capacity to make reliable predictions. This assumption is based on the premise that the transition from no wear to worn occurs with minimal time deviations. In practice, recognizing wear too late is undesirable. To mitigate this, the transition from ”not worn” to ”worn” could be adjusted slightly earlier in the labeling process, thereby introducing a calculated bias for the early prediction of

wear. Alternatively, if avoiding such a bias is preferred and high time accuracy is still desired, training on data from four or more tool life cycles becomes necessary.

These observations hold true when the models are applied to an identical process with the same machine. The next step is to examine the behavior of the trained models in relation to data from a different machine. For this, Fig. 8 illustrates the accuracy of the various model architectures, using a dataset from the DMU60FD machine. It should be noted that the

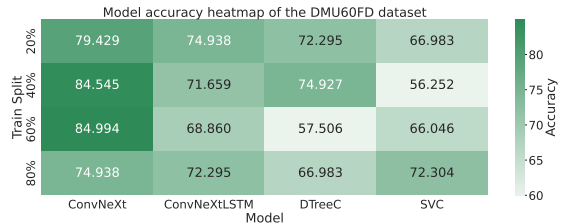


Fig. 8: A heatmap showing the accuracy of the different trained models on the DMU60FD dataset.

training data of the different splits are identical to those used in the heatmap in Fig. 6. It is evident that the models on the unseen machine exhibit reduced performance, yet the ConvNeXt model continues to demonstrate the most optimal outcomes. Interestingly, models trained with the largest dataset (80% training data) perform worse than those trained with smaller datasets. This suggests that the change of a machine has fundamentally altered the wear behavior, causing models trained on extensive data to overfit to the specific characteristics of the original machine. Models trained with 40% of the training data achieve the high-

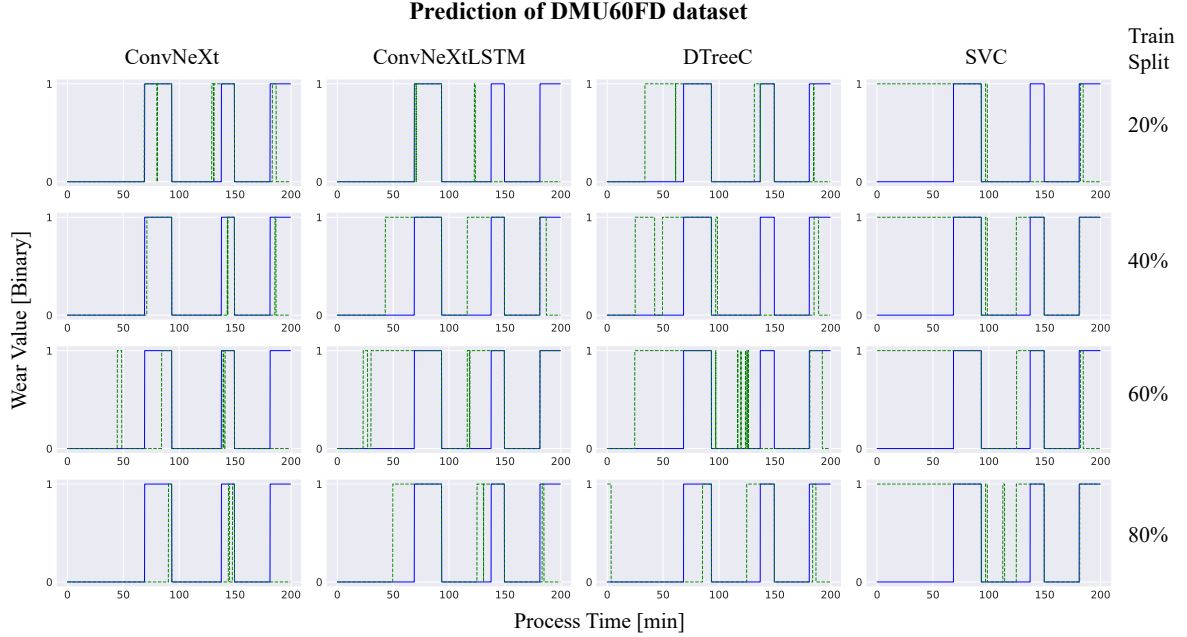


Fig. 9: The time-based wear predictions of the DMU60FD dataset. The dashed green line represents the model's predictions, while the blue line indicates the true labels.

est accuracy. An examination of the accuracy over time (Fig. 9) reveals that the models are capable of detecting changes in the DMU60FD dataset and successfully predict wear in some tool life cycles. Nevertheless, when considering all models collectively, while each tool life cycle is successfully recognized by at least one model, no single model achieves consistent accuracy across all cycles. This suggests that the findings derived from the training dataset can be applied to the DMU60FD dataset. However, no overarching patterns are identified that apply to all tool life cycles. In summary, the fundamental issue associated with TCM's is also clear in this study, namely that the complex characteristics of each machine make it difficult to implement one prediction model across other unseen machines. To improve predictions, the models require additional training data from the specific machine.

VI. CONCLUSION

This paper addresses the question of how to develop a TCM system that is transferable to industrial applications. For this, a modular approach and a non-invasive setup is employed so that a TCM can be installed for different milling processes with minimal effort. For a non-invasive setup, a 1D acceleration sensor is used, and for modality the sensor is integrated into a toolholder. In this research, the acceleration signal is processed in both the time domain and the frequency domain, to generate valuable data input for wear prediction or TCM. The best performing TCM approach uses short-time Fourier transform as input and an automatic feature extraction through CNN architecture to predict wear. Given that the development of a TCM

is more cost-effective when fewer training data are required, the study also investigates the amount of training data needed from a milling process to get a sufficient accuracy: To achieve the highest degree of accuracy in wear prediction, at least four tool life cycles should be included in the training data, two or three cycles for an acceptable accuracy. Among the models tested, the ConvNeXt model delivered the best results with 99% accuracy. Additionally, the models capacity to predict wear for an untrained milling machine is evaluated. Although models demonstrate some ability to transfer information and predict wear for certain tools, they struggle to fully capture the inherent complexity and variability of new milling machines, resulting in inconsistent wear predictions. Transfer learning will therefore be necessary for new processes. A potential next step is to investigate the quantity of data required for effective transfer learning.

DATA AVAILABILITY

The authors do not have permission to share data.

ACKNOWLEDGEMENTS

The authors would like to thank SCHUNK SE & Co. KG for their valuable support.

APPENDIX A
TABLES OF THIS RESEARCH

TABLE I: Feature names and their corresponding formulas

Feature Name	Formula / Description
Mean	$\frac{1}{N} \sum_{i=1}^N x_i$
RMS (Root Mean Square)	$\sqrt{\frac{1}{N} \sum_{i=1}^N x_i^2}$
SD (Standard Deviation)	$\sqrt{\frac{1}{N-1} \sum_{i=1}^N (x_i - \bar{x})^2}$
Crest Factor	$\frac{\max x }{\text{RMS}}$
Kurtosis	$\frac{1}{N} \sum_{i=1}^N \left(\frac{x_i - \bar{x}}{\text{SD}} \right)^4$
Skewness	$\frac{1}{N} \sum_{i=1}^N \left(\frac{x_i - \bar{x}}{\text{SD}} \right)^3$
Statistical Mode	Most frequent value in the dataset
SD of Statistical Mode	Standard deviation of the statistical mode
P2P (Peak-to-Peak)	$\max(x) - \min(x)$
Energy of Power Spectral Density (PSD)	$\sum_{n=1}^N X(f) ^2$, where $X(f)$ is the PSD of $x(t)$
Power Spectral Entropy	$-\sum_{n=1}^N P(n) \log_2 P(n)$, where $P(n)$ is the probability distribution of a power spectrum
Relative Energy of aperiodic frequencies	$\frac{\text{Energy}_{ap}}{\text{Energy}_{all}}$, where ap is energy of the aperiodic frequencies
Auto-correlation	$\frac{\sum_{i=1}^{N-\tau} (x_i - \bar{x})(x_{i+\tau} - \bar{x})}{\sum_{i=1}^N (x_i - \bar{x})^2}$
Higuchi Fractal Dimension	Linear regression on the points $\{(\log(1/k), \log(L(k)))\}$ to estimate the slope, where k is the interval length or scale parameter and $L(k)$ the curve length

TABLE II: Process parameters from the measured acceleration data for the models

Process Parameter	Value
Axial depth of cut (a_p)	12 mm
Radial depth of cut (a_e)	1.2 mm
Cutting speed (v_c)	435 m/min
Feed rate (v_f)	5540 mm/min
Feed per tooth (f_z)	0.12 mm
Spindle speed (n)	11540 rpm

REFERENCES

- [1] C.-H. Lim, M.-J. Kim, J.-Y. Heo, K.-J. Kim, Design of informatics-based services in manufacturing industries: Case studies using large vehicle-related databases 29 (3) 497–508. doi:10.1007/s10845-015-1123-8. URL <https://doi.org/10.1007/s10845-015-1123-8>
- [2] H. Zeng, R. Yan, P. Du, M. Zhang, F. Peng, Notch wear prediction model in high speed milling of AerMet100 steel with bull-nose tool considering the influence of stress concentration 408–409 228–237. doi:10.1016/j.wear.2018.05.024. URL <https://www.sciencedirect.com/science/article/pii/S0043164818301364>
- [3] H. Zhang, S. Jiang, D. Gao, Y. Sun, W. Bai, A Review of Physics-Based, Data-Driven, and Hybrid Models for Tool Wear Monitoring 12 (12) 833. doi:10.3390/machines12120833. URL <https://www.mdpi.com/2075-1702/12/12/833>
- [4] D. Y. Pimenov, A. Bustillo, S. Wojciechowski, V. S. Sharma, M. K. Gupta, M. Kuntoğlu, Artificial intelligence systems for tool condition monitoring in machining: Analysis and critical review doi:10.1007/s10845-022-01923-2. URL <https://link.springer.com/10.1007/s10845-022-01923-2>
- [5] G. Serin, B. Sener, A. M. Ozbayoglu, H. O. Unver, Review of tool condition monitoring in machining and opportunities for deep learning 109 (3) 953–974. doi:10.1007/s00170-020-05449-w. URL <https://doi.org/10.1007/s00170-020-05449-w>
- [6] R. Daicu, G. Oancea, Methodology for Measuring the Cutting Inserts Wear 14 (3) 469. doi:10.3390/sym14030469. URL <https://www.mdpi.com/2073-8994/14/3/469>
- [7] F. Bleicher, D. Biermann, W. G. Drossel, H. C. Moehring, Y. Altintas, Sensor and actuator integrated tooling systems 72 (2) 673–696. doi:10.1016/j.cirp.2023.05.009. URL <https://www.sciencedirect.com/science/article/pii/S0007850623001385>
- [8] U. Awasthi, Z. Wang, N. Mannan, K. R. Pattipati, G. M. Bollas, Physics-based modeling and information-theoretic sensor and settings selection for tool wear detection in precision machining 81 127–140. doi:10.1016/j.jmapro.2022.06.027. URL <https://www.sciencedirect.com/science/article/pii/S152661252200411X>
- [9] W. Li, H. Fu, Z. Han, X. Zhang, H. Jin, Intelligent tool wear prediction based on Informer encoder and stacked bidirectional gated recurrent unit 77 102368. doi:10.1016/j.rcim.2022.102368. URL <https://www.sciencedirect.com/science/article/pii/S0736584522000552>
- [10] Q. An, Z. Tao, X. Xu, M. El Mansori, M. Chen, A data-driven model for milling tool remaining useful life prediction with convolutional and stacked LSTM network 154 107461. doi:10.1016/j.measurement.2019.107461. URL <https://www.sciencedirect.com/science/article/pii/S0263224119313284>
- [11] R. Zhao, R. Yan, Z. Chen, K. Mao, P. Wang, R. X. Gao, Deep learning and its applications to machine health monitoring 115 213–237. doi:10.1016/j.ymssp.2018.05.050. URL <https://linkinghub.elsevier.com/retrieve/pii/S0888327018303108>
- [12] B. Li, T. Liu, J. Liao, C. Feng, L. Yao, J. Zhang, Non-invasive milling force monitoring through spindle vibration with LSTM and DNN in CNC machine tools 210 112554. doi:10.1016/j.measurement.2023.112554. URL <https://www.sciencedirect.com/science/article/pii/S0263224123001185>
- [13] A. Misal, H. Karandikar, S. Sayyad, A. Bongale, S. Kumar, V. Warke, Milling Tool Wear Estimation Using Machine Learning with Feature Extraction Approach, in: 2024 MIT Art, Design and Technology School of Computing International Conference (MITADTSoCiCon), pp. 1–7. doi:10.1109/MITADTSoCiCon60330.2024.10575626. URL <https://ieeexplore.ieee.org/document/10575626>
- [14] J. Wang, Z. Xiang, X. Cheng, J. Zhou, W. Li, Tool Wear State Identification Based on SVM Optimized by the Improved Northern Goshawk Optimization 23 (20) 8591. doi:10.390/s23208591. URL <https://www.mdpi.com/1424-8220/23/20/8591>
- [15] S. Bagri, A. Manwar, A. Varghese, S. Mujumdar, S. S. Joshi, Tool wear and remaining useful life prediction in micro-milling along complex tool paths using neural networks 71 679–698. doi:10.1016/j.jmapro.2021.09.055. URL <https://www.sciencedirect.com/science/article/pii/S1526612521007167>
- [16] Y. Cheng, M. Lu, X. Gai, R. Guan, S. Zhou, J. Xue, Research on multi-signal milling tool wear prediction method based on GAF-ResNext 85 102634. doi:10.1016/j.rcim.2023.102634. URL <https://www.sciencedirect.com/science/article/pii/S0736584523001096>
- [17] Z. Li, X. Liu, A. Incecik, M. K. Gupta, G. M. Królczyk, P. Gardoni, A novel ensemble deep learning model for cutting tool wear monitoring using audio sensors 79 233–249. doi:10.1016/j.jmapro.2022.04.066. URL <https://www.sciencedirect.com/science/article/pii/S1526612522003024>
- [18] G. Martínez-Arellano, G. Terrazas, S. Ratchev, Tool wear classification using time series imaging and deep learning 104 (9) 3647–3662. doi:10.1007/s00170-019-04090-6. URL <https://doi.org/10.1007/s00170-019-04090-6>
- [19] D. Peng, H. Li, Intelligent monitoring of milling tool wear based on milling force coefficients by prediction of instantaneous milling forces 208 111033. doi:10.1016/j.ymsp.2023.111033. URL <https://www.sciencedirect.com/science/article/pii/S088832702300941X>
- [20] K. Wang, A. Wang, L. Wu, G. Xie, Machine Tool Wear Prediction Technology Based on Multi-Sensor Information Fusion 24 (8) 2652. doi:10.3390/s24082652. URL <https://www.mdpi.com/1424-8220/24/8/2652>
- [21] L. Yingguang, L. Changqing, L. Dehua, H. Jiaqi, W. Peng, Tool wear dataset of nuaa_ideahouse (2021). doi:10.21227/3aa1-5e83. URL <https://dx.doi.org/10.21227/3aa1-5e83>
- [22] A. Agogino, K. Goebel, Nasa milling Dataset. URL <https://www.nasa.gov/intelligent-systems-division/disc-covery-and-systems-health/pcoe/pcoe-data-set-repository/>
- [23] Y.-C. Chen, 2010 PHM Society Conference Data Challenge. URL <https://iee-dataport.org/documents/2010-phm-society-conference-data-challenge>
- [24] M. Kiouss, A. Ouahabi, M. Boudraa, R. Serra, A. Cheknane, Detection process approach of tool wear in high speed milling 43 (10) 1439–1446. doi:10.1016/j.measurement.2010.08.014. URL <https://www.sciencedirect.com/science/article/pii/S0263224110001880>
- [25] C. Li, B. Li, H. Wang, D. Shi, F. Gu, A. D. Ball, Tool Wear Monitoring in CNC Milling Process Based on Vibration Signals from an On-Rotor Sensing Method, in: H. Zhang, Y. Ji, T. Liu, X. Sun, A. D. Ball (Eds.), Proceedings of TEPEN 2022, Springer Nature Switzerland, pp. 268–281. doi:10.1007/978-3-031-26193-0_23.
- [26] X. Zhang, C. Han, M. Luo, D. Zhang, Tool Wear Monitoring for Complex Part Milling Based on Deep Learning 10 (19) 6916. doi:10.3390/app10196916. URL <https://www.mdpi.com/2076-3417/10/19/6916>
- [27] X. Yang, R. Yuan, Y. Lv, L. Li, H. Song, A Novel Multivariate Cutting Force-Based Tool Wear Monitoring Method Using One-Dimensional Convolutional Neural Network 22 (21) 8343. arXiv:36366041, doi:10.3390/s22218343.
- [28] X. Cao, B. Chen, B. Yao, S. Zhuang, An Intelligent Milling Tool Wear Monitoring Methodology Based on Convolutional Neural Network with Derived Wavelet Frames Coefficient 9 (18) 3912. doi:10.3390/app9183912. URL <https://www.mdpi.com/2076-3417/9/18/3912>
- [29] H. Wang, M. Luo, F. Gu, Multi-domain Features Fusion Adaptive Neural Network Tool Wear Recognition Model, in: H. Zhang, Y. Ji, T. Liu, X. Sun, A. D. Ball (Eds.), Proceedings of TEPEN 2022, Springer Nature Switzerland, pp. 751–765. doi:10.1007/978-3-031-26193-0_66.
- [30] Z. Liu, H. Mao, C.-Y. Wu, C. Feichtenhofer, T. Darrell, S. Xie, A ConvNet for the 2020s. arXiv:2201.03545 [cs],

- doi:10.48550/arXiv.2201.03545.
URL <http://arxiv.org/abs/2201.03545>
- [31] K. He, X. Zhang, S. Ren, J. Sun, Deep residual learning for image recognition. arXiv:1512.03385[cs], doi:10.48550/arXiv.1512.03385.
URL <http://arxiv.org/abs/1512.03385>
- [32] Z. Liu, Y. Lin, Y. Cao, H. Hu, Y. Wei, Z. Zhang, S. Lin, B. Guo, Swin transformer: Hierarchical vision transformer using shifted windows. arXiv:2103.14030[cs], doi:10.48550/arXiv.2103.14030.
URL <http://arxiv.org/abs/2103.14030>
- [33] A. Dosovitskiy, L. Beyer, A. Kolesnikov, D. Weissenborn, X. Zhai, T. Unterthiner, M. Dehghani, M. Minderer, G. Heigold, S. Gelly, J. Uszkoreit, N. Houlsby, An image is worth 16x16 words: Transformers for image recognition at scale. arXiv:2010.11929[cs], doi:10.48550/arXiv.2010.11929.
URL <http://arxiv.org/abs/2010.11929>
- [34] E. Westphal, H. Seitz, A machine learning method for defect detection and visualization in selective laser sintering based on convolutional neural networks 41 101965. doi:10.1016/j.addma.2021.101965.
- [35] J. Runge, R. Zmeureanu, A Review of Deep Learning Techniques for Forecasting Energy Use in Buildings 14 (3) 608. doi:10.3390/en14030608.
URL <https://www.mdpi.com/1996-1073/14/3/608>